

Pharmaceutical compounds removal through pristine, alkali-, acid-, and layered double hydroxide-modified biochar: Characterization, kinetics, and isotherms studies

Zaidun Naji Abudi^{1*} , Yasir Talib Hameed¹, Alkhafaji R. Abood², Rasha Al-Saedi¹

¹ Department of Environmental Engineering, College of Engineering, Mustansiriyah University, Baghdad, 00964, Iraq

² Department of Civil Engineering, College of Engineering, University of Thi Qar, Nasiriyah, 00964, Iraq

* Corresponding author's e-mail: zaidun.naji77@uomustansiriyah.edu.iq

ABSTRACT

The negative impact of pharmaceuticals as emerging contaminants in water, as well as their effects in developing resistant genes to these medicines, has attracted the attention of researchers. In this study, biochar derived from agricultural waste was prepared and modified with acid, base, and layered double hydroxide, resulting in AWBC- H_3PO_4 , AWBC- KOH, and AWBC- LDH (Mg-Al), respectively, to investigate their adsorption capacities towards acetaminophen (ACT) removal from aqueous solution. Kinetics, isotherms, and characterization studies were also performed. The results showed an improvement in removal efficiencies in ACT using AWBC- LDH (Mg-Al), AWBC- KOH, and AWBC- H_3PO_4 (around 95%), compared to the un-modified biochar (85%) at a contact time of 150 min. This improvement enhanced the equilibrium uptake of the modified biochar (1.15–1.31 fold) compared to the raw biochar. The kinetic study proved that the pseudo-second order model could fit the data better (values of R^2 are more than 0.94), indicating that the process was mostly chemisorption. Isotherm studies indicated that the Langmuir model was preferable for all types of biochar (values of R^2 are more than 0.92), indicating monolayer adsorption. Most of the functional groups appearing in the FTIR of raw biochar remain in the modified biochar, indicating that the modification did not change the carbon skeleton of biochar. Moreover, SEM images showed a clear difference in the morphology of biochars' surfaces as a consequence of modifications. The outcome of this research shows the ability of this biochar to adsorb ACT and the effectiveness of modification methods to improve the removal efficiencies.

Keywords: biochar, adsorption, acetaminophen, activation, layer double hydroxides.

INTRODUCTION

The aquatic environment is facing a rapid increase in concentrations of various contaminants, particularly pharmaceutical compounds. The significant increase in their concentrations is due to the increase in population and wide use. Statistics report that around 6000 tons/year of tetracycline is consumed in the United States (Aliyu et al., 2022). Pharmaceuticals are excreted from the human and animal bodies with urine and feces, resulting in detectable concentrations in wastewater. They subsequently find their way to water resources through the discharge of wastewater. The improper disposal of leftover and expired

pharmaceuticals has also led to an increase in their concentrations in water resources (Sellaoui et al., 2023). Pharmaceuticals-loaded wastewater can be treated using biological, chemical, and physical processes. Different biological processes are being investigated to treat pharmaceutical wastewater, such as constructed wetlands (Jain et al., 2023), membrane bioreactors (Utami et al., 2024), and aerated filters (Abdullah et al., 2016; Chen et al., 2017). The chemical processes that are applied to remove pharmaceuticals from wastewater include coagulation (Jung et al., 2015), ozonation (Peralta-Hernández and Brillas, 2023), advanced oxidation (Qutob et al., 2022; Ramasamy et al., 2021), photo-Fenton process (Durán et al., 2011),

photocatalytic degradation (Nasr et al., 2019; Negarestani et al., 2020). Physical processes have also been employed to remove pharmaceuticals from wastewater, including membrane filtration, reverse osmosis (Karaman et al., 2016), and adsorption (Abudi et al., 2025; Nguyen et al., 2020). Removal of pharmaceuticals from wastewater should be fully managed at source, instead of focusing on the application and improvement of such treatment techniques, which are costly and unsustainable. Adsorption is favorable among these techniques as it is a cost-effective and environmentally friendly method (Abudi et al., 2025).

Various adsorbent materials have been tested for the treatment of pharmaceutical wastewater. Moving towards the sustainability concepts, adsorbents derived from natural materials have recently been encouraged. Biochar as an adsorbent has attracted much attention because it is cheap, sustainable, efficient, and abundant (Qasim et al., 2023). Biochar is a solid material originated thermally from organic matter decomposition under a low-oxygen sealed environment. The performance of biochar depends on its chemical and physical structure, such as ion exchangeability, pore size, and specific surface area (Du et al., 2023). However, the adsorption capacity of biochar could be enhanced by specific chemical and physical modification procedures, which significantly enlarge the surface area and porosity of the adsorbent (Qasim et al., 2023). Different modifications have been applied to biochar, including the addition of metals and carbonaceous materials, as well as steam activation (a physical green modification). One of the efficient but expensive methods is modification using some organic matter such as methanol (Du et al., 2023). However, the most common technique is acid/base modification, which produces modified biochar with high adsorption characteristics (Jin et al., 2014; Peng et al., 2017).

Effective parameters that have a vital role in biochar adsorption are pH, temperature, amount of adsorbent, concentration of pollutants, and contact time (Abudi et al., 2025; Qasim et al., 2023). The effective mechanisms that participate in biochar adsorption are electron donor/acceptor interactions, electrostatic interaction, surface complexation, pore filling, hydrophobic interactions, hydrogen bonding interactions, and ion exchange (Du et al., 2023).

Biochar has been derived from various raw materials such as banana peel (Patel et al., 2021),

microalgae biomass (González-Hourcade et al., 2022), macroalgae (Pimentel-Almeida et al., 2023) and used to remove paracetamol. The impact of biochar as an adsorbent modified through acid, base, and layered double hydroxide for the removal of acetaminophen from synthetic wastewater is still inadequately reported. In order to fill this knowledge gap, the primary goal of this study was to assess the morphological, physico-chemical, and textural properties using various biochar composites, including activated biochar, biochar synthesized with layered double hydroxides, biochar modified with phosphoric acid, and biochar activated with potassium hydroxide, employing Fourier transform infrared spectroscopy (FTIR), X-ray diffraction (XRD), energy-dispersive X-ray spectroscopy (EDS), scanning electron microscopy (SEM), and Brunauer-Emmett-Teller (BET). The second goal was to examine the adsorption performance of acetaminophen (ACT) using the biochar composites and apply the kinetic and isotherm adsorption models to investigate the variables that affect the removal rate of acetaminophen, such as pH, initial ACT concentration, adsorbent dosage, and contact time.

MATERIALS AND METHODS

Materials

Tree leaves were gathered from Mustansiriyah University campus, Baghdad, Iraq. The used chemicals: acetaminophen, phosphoric acid (H_3PO_4), potassium hydroxide (KOH), magnesium nitrate ($Mg(NO_3)_2 \cdot 6H_2O$), aluminum nitrate ($Al(NO_3)_3 \cdot 9H_2O$), sodium hydroxide (NaOH), and sulfuric acid (H_2SO_4), were all analytical grade reagents, obtained from Aladdin, Ind., China, Shanghai. The stock solution of synthetic wastewater was provided by dissolving 1000 mg/L of ACT concentration in deionized water (DI) and then stored at 4 °C. This solution was diluted to the desired concentrations prior each experiment.

Synthesis of agricultural waste biochar

The collected leaves were washed properly with tap water and then with DI. The second step was drying the cleaned leaves using an air oven at 105 °C for 24 hours. The dried leaves were then grounded and sieved using a 0.2 mm sieve. The powder passed through the sieve was collected

in an iron box with dimensions of $30 \times 20 \times 40$ cm. The final step is the pyrolysis process in which the iron box is exposed to a high temperature ($360\text{ }^{\circ}\text{C}$) for 1 h under limited oxygen conditions using a temperature-controlled furnace at a heating speed of $10\text{ }^{\circ}\text{C}/\text{min}$ (Qasim et al., 2023). Thereafter, the agricultural waste biochar (AWBC) was identified using FTIR, XRD, EDS, SEM, and BET analyses. The residual biochar was preserved for more modifications.

Modification of biochar

Three methods were used to modify biochar in order to improve its characteristics. The first method was acid modification using phosphoric acid (H_3PO_4), the second method was base modification using potassium hydroxide (KOH), and the last one was layered double hydroxides (AWBC-LDH (Mg-Al)).

Modification of biochar with H_3PO_4 (AWBC- H_3PO_4)

Modification of AWBC by phosphorus acid was carried out by the impregnation of biochar in 47.5% phosphoric acid solution for 24 h at room temperature. The weight ratio of impregnation (acid solution: biochar) was 1:1. Then, the sample was subjected to drying (overnight at $60\text{ }^{\circ}\text{C}$) and pyrolysis under a nitrogen atmosphere at $600\text{ }^{\circ}\text{C}$ for 2 h. The sample was washed with DI after cooling, to ensure the removal of excessive phosphoric acid (within the pH value of 5.5–6.0). The sample was then dried, grounded, and passed through a 0.2 mm sieve (Peng et al., 2017). The obtained biochar (AWBC- H_3PO_4) was preserved in a sealed vessel and later analyzed with FTIR, XRD, EDS, SEM, and BET.

Modification of biochar with KOH (AWBC-KOH)

Modification of AWBC with potassium hydroxide was performed through mixing 2 g of AWBC with 500 ml of 2 M KOH solution for 1 h. Then, the mixed solution was filtered using filter paper. The filtered biochar was washed with DI and re-filtered. The process of washing and filtration was repeated several times until no significant change in the pH of the filtrate was noticed. The sample was then oven dried at $105\text{ }^{\circ}\text{C}$ for 10 h and pyrolyzed under an atmosphere of nitrogen at $600\text{ }^{\circ}\text{C}$ for 2 hr. The sample was washed after cooling with DI (ensuring the removal of excessive KOH), dried, grounded, and sieved using a

0.2 mm sieve (Jin et al., 2014). The biochar treated with KOH (AWBC-KOH) was preserved using a sealed vessel and subjected to FTIR, XRD, EDS, SEM, and BET analyses.

Modification of biochar with layered double hydroxides (AWBC-LDH (Mg-Al))

Biochar has a weak affinity towards the anionic compounds, because of its negative surface charge. In order to improve the biochar capacity to absorb such compounds, the biochar surface should be modified. It has been shown that adding layer double hydroxides (LDH (Mg-Al)) to the biochar improved its capacity to absorb anionic substances (Fang et al., 2018). The coprecipitation was performed following the procedure implemented by Xue et al. (2016) to produce biochar with layered double hydroxides (AWBC-LDH (Mg-Al)) (Xue et al., 2016). In brief, 100 mL (0.25M $\text{Al}(\text{NO}_3)_3 \cdot 9\text{H}_2\text{O}$) and 100 mL (0.75M $\text{Mg}(\text{NO}_3)_2 \cdot 6\text{H}_2\text{O}$) were combined. Once the mixture was shaken for an hour, 2.5 g of AWBC was added. When the shaking period finished, 2M NaOH was added to the mixture to bring the pH to about 10. Thereafter, the mixture was continually stirred for 10 hours at $85\text{ }^{\circ}\text{C}$. Following an oven-drying process for 24 hours at $100\text{ }^{\circ}\text{C}$, the precipitate (AWBC-LDH (Mg-Al)) was preserved in a sealed vessel and subsequently subjected to FTIR, XRD, EDS, SEM, and BET analyses.

Characterization of biochar

The characteristics of AWBC and its modifications were analyzed before the adsorption process. Functional groups were determined by FTIR test, elemental analysis was done by energy-dispersive X-ray spectroscopy (EDX), the crystal-line structure was analyzed by XRD, surface area, pore size, and pore volume were determined by BET analysis. Biochar structure was observed by scanning electron microscopy (SEM).

Batch adsorption experiments

In order to examine the ACT adsorption from aqueous solution using different biochar composites, the adsorption experiments were conducted on a batch basis. Each bottle (250 mL glass) was filled with 100 mL of pharmaceutical synthetic wastewater. The bottles were shaken using a reciprocating shaker at 200 rpm under ambient temperature. The investigated

parameters were pH (2–12), amended with 0.1M NaOH or 0.1M H₂SO₄), contact time (5–150 min), ACT initial concentration (40–200 mg/l), and the dose of adsorbent (0.1–1.1 g). Other factors were fixed to determine the impact of a particular factor.

For one experiment, the solution was filtered after a specified duration of contact time, and a spectrophotometer was used to measure ACT concentrations in the resultant liquid. Residual paracetamol in the synthetic wastewater after the adsorption experiments was analyzed by UV-visible spectrophotometer at 243 nm. The average of the data was taken and displayed after the samples were tested in duplicate. Equations 1 and 2 were applied to determine the quantity of the adsorbed ACT and the removal percentage, respectively:

$$q_e = \frac{V \cdot (C_{in} - C_e)}{m} \quad (1)$$

$$\% \text{Removal} = \frac{(C_{in} - C_{out})}{C_{in}} \cdot 100\% \quad (2)$$

where: q_e (mg/g) – quantity of the adsorbed ACT/unit mass of biochar; C_{in} (mg/L) – initial ACT concentration; C_{out} (mg/L) – ACT concentration at time (t); V (L) – solution volume; C_e (mg/L) – ACT concentration in solution at equilibrium; and m (g) – mass of biochar.

Kinetic study

Pseudo-first and second order kinetic models were employed to analyze the adsorption reaction of the applied initial ACT concentrations for the purpose of identifying the ACT adsorption route. Equations 3 and 4, respectively, provide a mathematical description of these models:

$$\frac{dq}{dt} = K_1 (q_e - q_t) \quad (3)$$

$$\frac{dq}{dt} = K_2 (q_e - q_t)^2 \quad (4)$$

where: q_e and q_t , expressed in mg/g, show the quantity of ACT adsorbed at equilibrium and at time t (minute), respectively, per unit mass of biochar. In the pseudo-first-order model, K_1 is a constant that shows the rate of sorption at equilibrium ($\text{g mg}^{-1} \text{min}^{-1}$). In the pseudo-second-order model, α is the initial rate of adsorption ($\text{mg/g} \cdot \text{min}$), β is the constant of desorption, and K_2 is the rate constant ($\text{g mg}^{-1} \text{min}^{-1}$).

Isotherm study

Freundlich, Langmuir, and Tempkin were used as adsorption isotherms to understand the connection between amount of adsorbate and concentration and determine the influence of initial ACT concentration on adsorption of the biochar composites (Zhu et al., 2018). Understanding the dynamic function of adsorption relies greatly on the adsorption isotherms. The Freundlich, Langmuir, and Tempkin isotherms are shown in Equations 5, 6, and 7 respectively:

$$\ln qe = \ln k_f + \frac{1}{n} \ln Ce \quad (5)$$

$$\frac{c_e}{q_e} = \frac{1}{k_l q_{max}} + \frac{c_e}{q_{max}} \quad (6)$$

$$qe = \frac{RT}{BT} \ln K_T + \left(\frac{RT}{BT}\right) \ln Ce \quad (7)$$

where: q_e – mass of ACT adsorbed per unit biochar; k_f and n – capacity factor and Freundlich intensity constant, respectively; q_{max} – mass of adsorbed ACT to complete saturation of the biochar unit mass (mg/g); C_e – ACT equilibrium concentration in solution after adsorption (mg/L); B_T – constant of Tempkin isotherm (J mol^{-1}); B – constant of experiment; T – absolute temperature; K_T – Tempkin constant at equilibrium binding (L/g); and R – gas constant (8.314 J mol^{-1}).

Statistical analysis

The average, standard deviation, and correlation coefficient were calculated using excel software (MS 2016). The figures were generated using the software of Origin Pro 2021.

RESULTS AND DISCUSSIONS

Characterization of biochar

Characterization of AWBC and its modifications was conducted before the adsorption process using FTIR, XRD, EDX, BET, and SEM analyses. Figure 1 shows the FTIR results of the biochar composites. Regarding AWBC, the band at 3414 cm^{-1} could be correlated to the stretching of O-H. Bands at 2922 and 2852 cm^{-1} are ascribed to the stretching of C-H. Peaks at 1703 cm^{-1} are a consequence of C=O stretching, while C=C stretching vibration is reflected at 1612 cm^{-1} . Peaks at

1444, 1361, 885, 831, and 779 cm^{-1} are ascribed to the C-H bending, whereas peaks at 1315, 1161, 1107, and 1060 cm^{-1} are correlated to stretching vibration of C-O. Peaks at 596, 513, and 437 cm^{-1} are attributed to the bending of O-H. Appearance of multiple peaks at the same functional group, suggesting the presence of this functional group within various compounds, which is anticipated in biochar derived from natural materials like agricultural waste.

Regarding AWBC- H_3PO_4 , the peak at 3379 cm^{-1} is attributed to the stretching of O-H. A clear diminution of this peak in comparison with the peak of AWBC, indicating the dehydration phenomenon (Peiris et al., 2019). The peak at 2951 cm^{-1} is a reflection of C-H stretching, whereas peaks at 1625 and 1527 cm^{-1} are linked to the stretching vibration of C=C. The peaks at 1442 and 1404, 995 and 885 cm^{-1} are connected to the C-H bending. The effect of modification with phosphoric acid is appeared at 1136 cm^{-1} as a stretching of P-O, revealing the successful modification and the embedment of phosphorus in the chemical structure of biochar (Chen et al., 2022). This result agrees with the results of EDX shown in Fig. 3, which indicates a high percentage of phosphorus among other elements in AWBC- H_3PO_4 .

It can be indicated from Figure 1 that the functional groups of AWBC-KOH are relatively close to those of AWBC. The peak at 3450 cm^{-1} is related to the O-H stretching, whereas the peak at 2904 cm^{-1} is a reflection of C-H stretching. The

peak at 1637 cm^{-1} is linked to the stretching vibration of C=C, whereas the peaks at 1379, 947, 869, and 779 cm^{-1} are ascribed to the bending of C-H.

The functional groups appearing in the FTIR results of AWBC-LDH (Mg-Al) are similar to a certain extent to the functional groups appearing in the FTIR of AWBC-KOH. The peak at 3415 cm^{-1} is owing to the stretching vibration of O-H (Wang et al., 2020), while 2926 and 2850 cm^{-1} peaks are connected to the C-H stretching. The peaks at 1716 cm^{-1} indicates the stretching of C=O, and 1635 cm^{-1} is linked to the C=C stretching. The peaks at 1377 and 1109 cm^{-1} are related to the bending of C-H (Wang et al., 2020).

Although the effect of modification (by KOH and layered double hydroxides) on the appearance of new functional groups was not clear; it may appear with the increase or decrease in the intensity of specific peaks or shifting in their positions. The same phenomenon was noticed by Ding et al. (2024). In general, most of the functional groups in the results of AWBC appeared the same in those with the biochar composites, such as C-H, O-H, C=C stretching, and C-H bending, highlighting the fact that the carbon skeleton of biochar did not change post to modification (Chen et al., 2022).

The results of XRD analysis of biochar composites are shown in Figure 2. The XRD spectra of AWBC showed that its main composition was crystalline cellulose, represented at $2\theta = 15.19^\circ$ (Wen et al., 2022). The strong absorption peak at $2\theta = 24.63^\circ$ and 25.59° could be attributed to the existence of graphite (Zhang et al., 2022). The

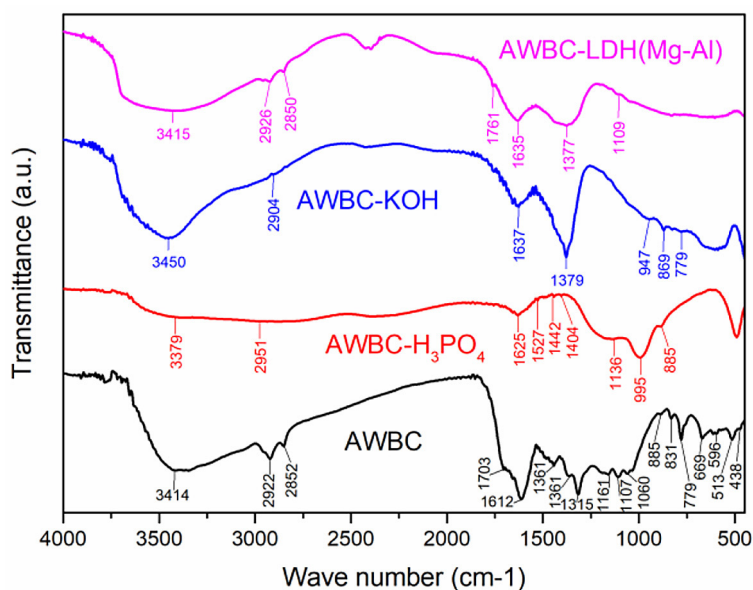


Figure 1. FTIR for AWBC and its three modifications

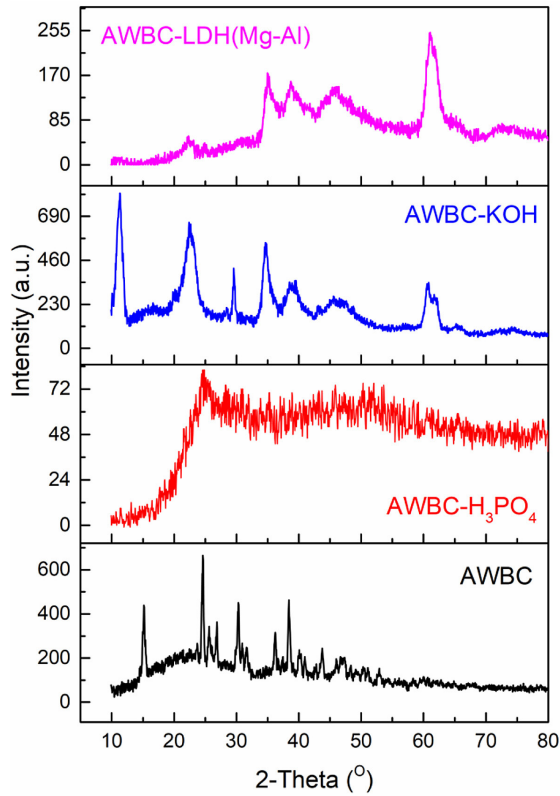


Figure 2. XRD for AWBC and its three modifications

peak at $2\theta = 26.9^\circ$ may represent the existence of silicon oxide (Chang et al., 2021). The peaks at $2\theta = 30.32$ and 31.62 are correlated to calcium-based compounds, whereas the peak at $2\theta = 36.217$ is

ascribed to silicon oxide (Hamid et al., 2022). Peak at $2\theta = 38.38$ is attributed to calcium oxide (Zhang et al., 2022).

The peaks in the XRD spectra of AWBC disappeared from those of AWBC- H_3PO_4 , and hence the results of AWBC- H_3PO_4 did not show distinct peaks. This is due to the ability of H_3PO_4 to promote the amorphous carbon and change the crystalline structure (Chen et al., 2022). The results of AWBC-KOH showed a similar pattern as AWBC, indicating the neglected impact of the modification process on the AWBC structure, although some changes were expected from the addition of potassium. The XRD of AWBC-LDH (Mg-Al) showed a peak of $2\theta = 34.9$, attributable to the magnesium compounds (Wen et al., 2022), while $2\theta = 38.74$ and 61.07 could be related to aluminum oxide. These results showed a significant change in the crystallinity of AWBC structure after modification by layered double hydroxides, with the embedment of magnesium and aluminum in the biochar structure. The same phenomena was noticed by Wang et al. (2020) when a combined of Ni-Fe-Zn layered double hydroxides was used to modify the corn stalks biochar.

As shown in Figure 3, the main constituents of AWBC are carbon (50%) and oxygen (36%) in addition to the minor elements. In AWBC- H_3PO_4 , the main constituents are oxygen (46%) and phosphorus (35%). The phosphorus increment was due

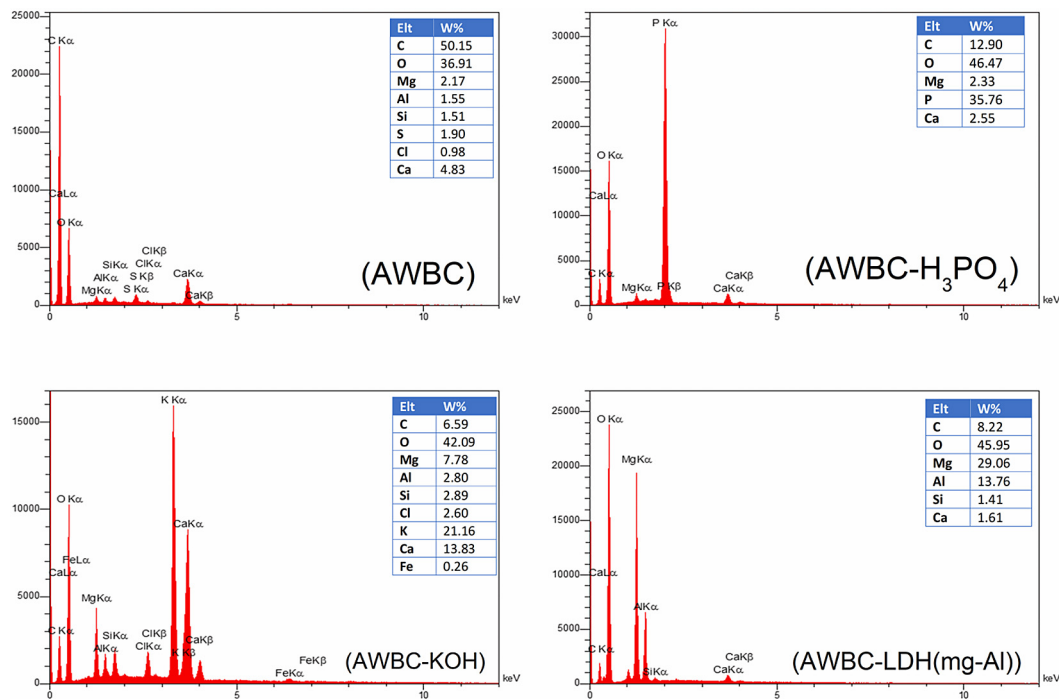


Figure 3. EDX for AWBC and its three modifications

to the modification of phosphoric acid, while the carbon percentage declined to 13% in comparison with AWBC. Oxygen, magnesium, and aluminum increased to 46%, 29%, and 13%, respectively, in AWBC-LDH (Mg-Al), compared to AWBC, whereas carbon decreased to 8%. This significant increment in the percentage of magnesium and aluminum is justified by the addition of these two elements during the modification process. In AWBC-KOH, the percentage of oxygen and potassium increased to 42% and 21%, respectively, but the carbon percentage decreased to 7% compared to AWBC. It is obvious that the biochar modification by KOH is behind the increment in potassium.

The results of SEM (Figure 4) show a clear difference in the morphology of these four types of biochar. Although the surface of raw biochar seems irregular, it is relatively smooth for AWBC- H_3PO_4 ;

which is in agreement with observations found by Chen et al. (2022). AWBC-KOH has a surface-like sheet, indicating a significant change in surface morphology from the modification with KOH; which is in accordance with the phenomenon noticed by Lee et al. (2021). A rough surface was observed in AWBC-LDH (Mg-Al), highlighting the presence of Mg/Al-LDHs that are dispersed on the biochar surface (Peng et al., 2021).

Results of pore size indicate that the majority of pores in all types of biochar are mesopores (2–50 nm), with no significant increment in pore size after the modifications. Pore volume did not also show a clear increment after modifications (0.055, 0.0714, 0.036, and 0.0349 cm^3/g for AWBC, AWBC-KOH, AWBC- H_3PO_4 , and AWBC-LDH (Mg-Al), respectively). The surface area of AWBC was 5.6498 m^2/g , with a potential improvement

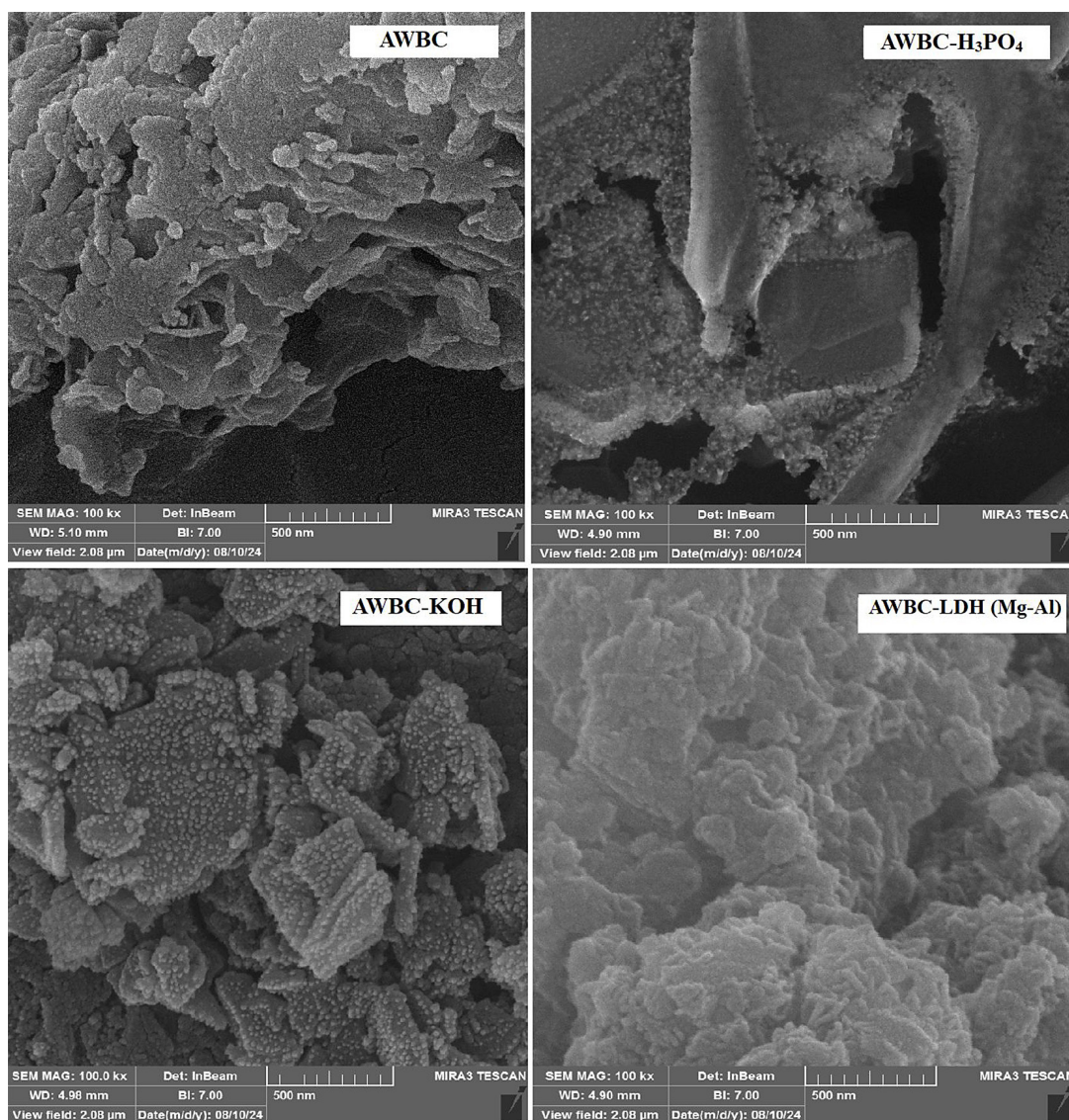


Figure 4. SEM for AWBC and its three modifications

in surface area of AWBC-KOH (17.188 m²/g), AWBC-LDH (Mg-Al) (11.466 m²/g), and AWBC-H₃PO₄ (16.837 m²/g). This coincided with the enhancement of the adsorption process, highlighting the contribution of the electrostatic adsorption mechanism (Chen et al., 2022). However, these values are considered small compared to other types of biochar (Liu et al., 2022).

Effect of pH

The impact of pH on the ACT removal rate from aqueous solution using AWBC, AWBC-H₃PO₄, AWBC-KOH, and AWBC-LDH (Mg-Al) was investigated. The results showed that alkaline pH dramatically deteriorates the removal efficiency of acetaminophen (Figure 5). The optimum pH value was 6 for AWBC, AWBC-H₃PO₄ and AWBC-KOH with removal efficiencies of 55, 88, and 78% respectively, while it was 8 for AWBC-LDH (Mg-Al), with removal efficiency of 80%. The optimum pH for acetaminophen adsorption in this study is comparable to that of acetaminophen adsorption on silica microspheres, which was 5 with a removal efficiency of 95%. Lower or higher than pH value of 5 significantly deteriorated the removal efficiency (Natarajan et al., 2021). On the other hand, different behavior was noticed when acetaminophen was adsorbed on banana peel biochar, where the acidic environment was preferable over the alkali environment (Patel et al., 2021). However, different adsorbent materials and modification methods might result

in different adsorption mechanisms and responses to various pH values. The clear effect of pH indicates that the electrostatic attraction mechanism has a vital role in the adsorption process (dos Reis et al., 2022). Moreover, the improvement in removal efficiencies of modified biochar confirmed the positive effect of modification on biochar performance.

Effect of adsorbent dose

A wide range of adsorbent doses were investigated for the AWBC and its modifications, and the results are depicted in Figure 6. The adsorption process enhanced as the adsorbent dose increased. For AWBC and its three modifications, at a dose of 0.1g, the removal efficiencies were around 40%, approaching 90% at a dose of 1.1g; however; little improvement in the removal rate was noticed when the adsorbent dose was between 0.9 to 1.1g, indicating no necessity for investigating such a higher dose. Furthermore, at high doses (0.9 and 1.1g), the performance of the modified biochar was clearly higher than the raw biochar. Various adsorbent doses were investigated by other researchers under different experimental conditions. Maneewong et al. (2022) used 0.08 g/100 ml of activated carbon derived from coconut shell to treat an aqueous solution containing 2000 mg/L of acetaminophen. dos Reis et al. (2022) used 0.15 g/100 ml of tree bark residue to treat acetaminophen (70–1200 mg/L) from an aqueous solution.

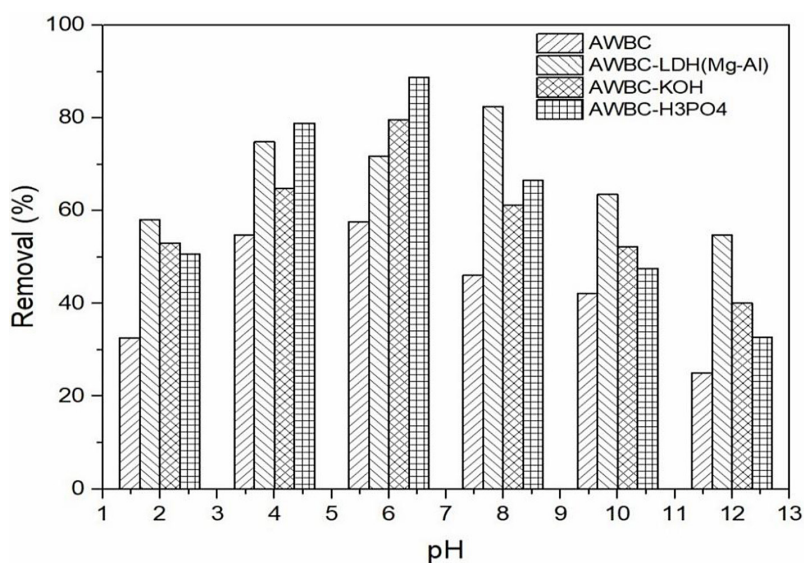


Figure 5. Effect of pH on removal efficiency of acetaminophen (initial concentration = 80 mg/L, dose of biochar = 0.3 g, time of contact = 150 min)

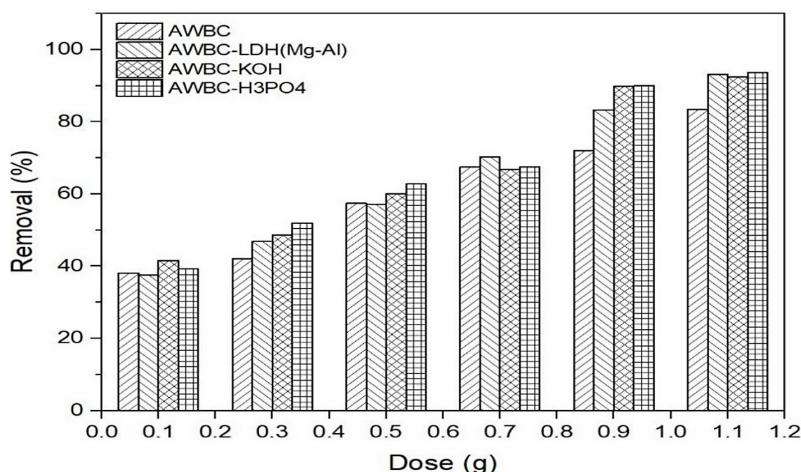


Figure 6. Effect of biochar dose on removal efficiency of acetaminophen (initial concentration = 80 mg/L, time of contact = 150 min, pH = 6 for AWBC, AWBC- KOH, AWBC- H₃PO₄ samples while pH = 8 for AWBC- LDH (Mg-Al)

Effect of acetaminophen initial concentration

The uptake of acetaminophen by AWBC and its modifications is depicted in Figure 7. Generally, at low concentrations of acetaminophen (40, 60, and 80 mg/l), the removal efficiency was high,

indicating that biochar and modifications had the ability to uptake this quantity of acetaminophen, and higher initial concentrations of acetaminophen are worth of being investigated. At concentrations higher than 80 mg/L, the removal efficiencies significantly declined, revealing that the biochar and

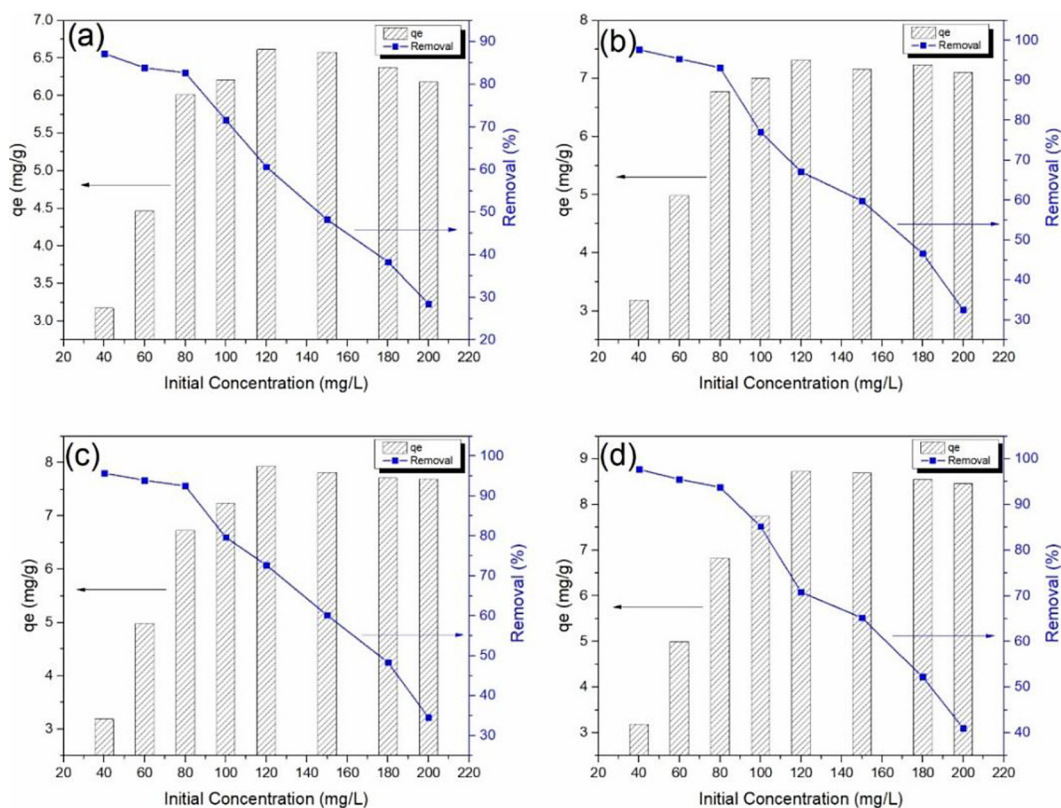


Figure 7. Effect of acetaminophen initial concentration on the uptake of acetaminophen at equilibrium (q_e) and removal efficiency, (a) AWBC (b) AWBC- LDH (c) AWBC- KOH (d) AWBC- H₃PO₄ (dose of biochar = 1.1 g, time of contact = 150 min, pH = 6 for AWBC, AWBC- KOH, AWBC- H₃PO₄ samples while pH = 8 for AWBC- LDH (Mg-Al)

modifications approached the saturation point. At 120 mg/L, the equilibrium uptake (q_e) reached the maximum, with a noticeable effect of biochar modification on the enhancement of q_e (6.5, 7.5, 7.5, 8.5 mg/g for AWBC, AWBC- LDH (Mg-Al), AWBC- KOH and AWBC- H_3PO_4 respectively). At concentrations higher than 120 mg/L, the removal efficiencies decreased dramatically since there was no more ability to uptake. However, the obtained equilibrium uptake (q_e) is significantly lower than that of other materials investigated by Maneewong et al. (2022), who obtained q_e values of around 200 mg/g for a coconut shell-based biochar. dos Reis et al. (2022) obtained more than 200 mg/g for a tree bark-based adsorbent. However, this significant difference could be justified by the difference in characteristics of raw materials and experimental conditions.

Effect of contact time

Figure 8 shows the influence of contact time on the removal efficiency of acetaminophen. The removal rate increased significantly as the contact time increased, indicating that more than 120 min is required to achieve greater than 90% removal. Moreover, the modification of biochar substantially enhanced the removal rate, particularly more than 60 minutes contact time. At the beginning of the experiment, the available free pores promoted the adsorption process; however, after

120 minutes, the removal efficiency declined, because of the pores saturation. A slow adsorption of acetaminophen was noticed by Loc et al. (2023), whereas dos Reis et al. (2022) did not notice the same behavior for tree bark-derived biochar, by which adsorption proceeded very fast, approaching an equilibrium state within the first few minutes. Fast adsorption generally results from the mechanism of surface adsorption and high affinity between acetaminophen molecules and biochar active sites, while slow adsorption indicates that pore filling is the main mechanism of adsorption (Loc et al., 2023).

Kinetic and isotherm studies

The kinetic models of pseudo-first and second order were applied to evaluate mathematically the adsorption process using kinetic parameters (Table 1). Values of R^2 in pseudo second order were higher (0.9481, 0.9412, 0.94, 0.9442 for AWBC, AWBC- LDH (Mg-Al), AWBC- KOH, and AWBC- H_3PO_4 respectively) than those of pseudo-first order (0.9155, 0.9003, 0.9264, 0.927 respectively), indicating that pseudo-second order suited better the kinetic data. The model also expressed the adsorption process more efficient than pseudo first order model. Pseudo-second order reveals that the process is mostly chemisorption and the abundance of active sites on the biochar surface had a key role in the determination of the

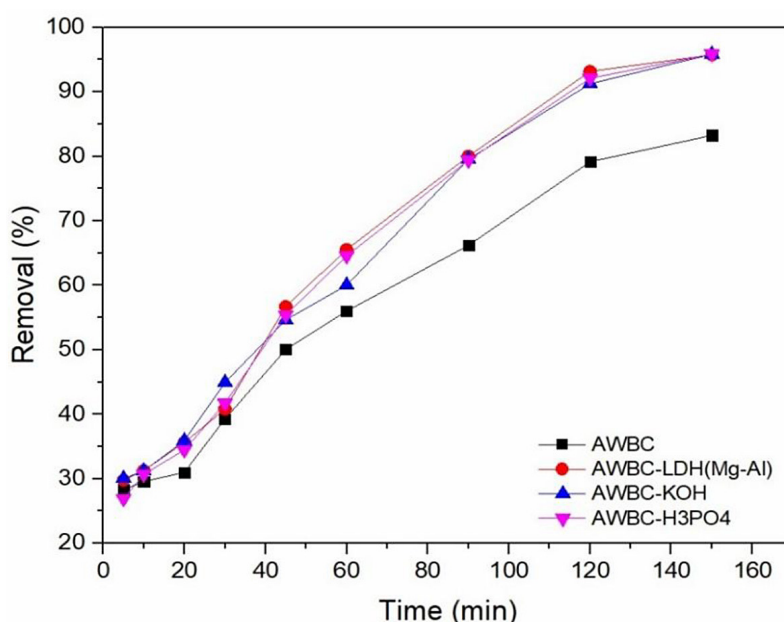


Figure 8. Effect of contact time on removal efficiency of acetaminophen (initial concentration = 120 mg/L, dose of biochar = 1.1 g, pH =6 for AWBC, AWBC- KOH, AWBC- H_3PO_4 samples while pH = 8 for AWBC- LDH (Mg-Al))

Table 1. Kinetics study parameters

Adsorbent	Experimental parameter		Pseudo-first order			Pseudo-second order		
	pH	q_e , exp (mg/g)	k_1 (1/min)	q_e , cal. (mg/g)	R^2	k_2 (g/mg/min)	q_e , cal. (mg/g)	R^2
AWBC	6	9.0841	0.021	8.335	0.9155	0.003	10.593	0.9481
AWBC- LDH (Mg-Al)	8	10.4440	0.026	11.242	0.9003	0.002	12.723	0.9412
AWBC- KOH	6	10.4566	0.022	10.178	0.9264	0.002	12.469	0.94
AWBC- H ₃ PO ₄	6	10.4591	0.024	10.766	0.927	0.002	12.771	0.9442

Table 2. Isotherm study parameters

Adsorbent	Langmuir isotherm				Freundlich isotherm			Tempkin isotherm		
	KL (L/mg)	q_m , cal. (mg/g)	R^2	RL	KF	n	R^2	KT	B	R^2
AWBC	0.036	17.182	0.933	0.424	1.485	1.953	0.893	0.263	4.201	0.8683
AWBC- LDH (Mg-Al)	0.287	9.737	0.9882	0.205	5.137	6.609	0.92	48.606	1.181	0.894
AWBC- KOH	0.146	13.643	0.9329	0.289	4.264	3.679	0.8674	2.444	2.546	0.8246
AWBC- H ₃ PO ₄	0.139	14.728	0.9216	0.295	4.231	3.391	0.8923	2.014	2.861	0.8346

adsorption capacity (Lessa et al., 2018). Moreover, low values of K_2 indicated a slow adsorption process (Figure 4), which were close to the K_2 values calculated by Lung et al. (2021), while dos Reis et al. (2022) showed relatively high K_2 values, signifying the fast adsorption mechanism of acetaminophen using an adsorbent derived from tree bark.

The isotherms of adsorption were studied using the Langmuir, Freundlich, and Tempkin models. Table 2 demonstrates the parameters of these models. Values of R^2 in Langmuir (0.933, 0.9882, 0.9329, 0.9216 for AWBC, AWBC- LDH (Mg-Al), AWBC- KOH, and AWBC-H₃PO₄ respectively) were higher than those in Freundlich and Tempkin, revealing that the Langmuir model fitted better the isotherm data and described the adsorption process. The same observation was noticed by Kerckhoff et al. (2021). Generally, the Langmuir model testifies monolayer adsorption, whereby the adsorbed molecules do not interact with each other (Quesada et al., 2019), with a homogenous adsorbent surface (Lung et al., 2021). The Freundlich formula showed less correlation to the experimental data, compared to the Langmuir and Tempkin model (R^2 was 0.893, 0.92, 0.8674, 0.8923 for AWBC, AWBC- LDH (Mg-Al), AWBC- KOH, and AWBC-H₃PO₄ respectively). In fact, the assumptions of Freundlich certify the multilayered adsorption and heterogeneity of the adsorbent surface, which is applicable to an extent since the values of R^2 were not very low (Lung et al., 2021).

CONCLUSIONS

The adsorption process successfully removed acetaminophen from the aqueous solution, and modification of the biochar showed a noticeable enhancement in the adsorption process (removal efficiency of acetaminophen using the AWBC was 85% compared to around 95% for the three modified biochar), corresponding with the significant increment in the surface area of the modified biochar compared to the raw biochar. Characterization of biochar indicated that the modification processes did not change the carbon skeleton of AWBC. However, SEM images showed a clear difference in the morphology of biochars' surfaces as a consequence of modifications.

The equilibrium uptake (q_e) of the modified biochar increased by 1.15–1.31-fold compared to the raw biochar. Modification of biochar improved significantly the ACT removal efficiency, in particular at a contact time of more than 60 minutes, achieving higher than 90% removal after 120 minutes of contact time.

Studies in kinetics showed that the pseudo-second order model best suited the kinetic data and described the adsorption process, highlighting that the process was mostly chemisorption and the active sites abundance on the biochar surface had a vital role in the determination of the adsorption capacity. The isotherm study demonstrated a favored adsorption with the Langmuir model to the other investigated models, indicating a monolayer

adsorption with no interaction between the adsorbed molecules. However, the Freundlich formula showed less correlation with the experimental data in comparison with the Langmuir model, verifying the multilayered adsorption and the heterogeneity of the adsorbent surface.

Finally, AWBC as an environmentally friendly adsorbent, showed a promising performance in removing acetaminophen from aqueous solution, and the modified biochar samples showed a noticeable improvement in terms of acetaminophen removal, which was justified by the enhancement of their characteristics.

Acknowledgments

The authors would like to thank Mustansiriyah University (www.uomustansiriyah.edu.iq) Baghdad – Iraq and the University of Thi Qar (<https://utq.edu.iq/>) Thi Qar-Iraq for their support in the present work.

REFERENCES

1. Abdullah, N., Fulazzaky, M. A., Yong, E. L., Yuzir, A., Sallis, P. (2016). Assessing the treatment of acetaminophen-contaminated brewery wastewater by an anaerobic packed-bed reactor. *Journal of environmental management*, 168, 273–279.
2. Abudi, Z. N., Al-Saedi, R., Abood, A. R. (2025). Adsorptive uptake of acetaminophen by agricultural waste-derived hydrochar: kinetics, isotherms, and characterization studies. *Sustainability*, 17(5), 1923. <https://www.mdpi.com/2071-1050/17/5/1923>
3. Aliyu, M., Abdullah, A. H., bin Mohamed Tahir, M. I. (2022). Adsorption tetracycline from aqueous solution using a novel polymeric adsorbent derived from the rubber waste. *Journal of the Taiwan Institute of Chemical Engineers*, 136, 104333.
4. Chang, C., Liu, Z., Li, P., Wang, X., Song, J., Fang, S., Pang, S. (2021). Study on products characteristics from catalytic fast pyrolysis of biomass based on the effects of modified biochars. *Energy*, 229, 120818.
5. Chen, J., Liu, Y.-S., Zhang, J.-N., Yang, Y.-Q., Hu, L.-X., Yang, Y.-Y.,... Ying, G.-G. (2017). Removal of antibiotics from piggery wastewater by biological aerated filter system: treatment efficiency and biodegradation kinetics. *Bioresource Technology*, 238, 70–77.
6. Chen, K., Ma, D., Yu, H., Zhang, S., Seyler, B. C., Chai, Z., Peng, S. (2022). Biosorption of V(V) onto Lantana camara biochar modified by H_3PO_4 : Characteristics, mechanism, and regenerative capacity. *Chemosphere*, 291, 132721.
7. Ding, J., Liang, J., Wang, Q., Tan, X., Xie, W., Chen, C.,...Chen, X. (2024). Enhanced tetracycline adsorption using KOH-modified biochar derived from waste activated sludge in aqueous solutions. *Toxics*, 12(10), 691.
8. dos Reis, G. S., Guy, M., Mathieu, M., Jebrane, M., Lima, E. C., Thyrel, M.,...Larsson, S. H. (2022). A comparative study of chemical treatment by $MgCl_2$, $ZnSO_4$, $ZnCl_2$, and KOH on physicochemical properties and acetaminophen adsorption performance of biobased porous materials from tree bark residues. *Colloids and Surfaces A: Physicochemical and Engineering Aspects*, 642, 128626.
9. Du, L., Ahmad, S., Liu, L., Wang, L., Tang, J. (2023). A review of antibiotics and antibiotic resistance genes (ARGs) adsorption by biochar and modified biochar in water. *Science of the Total Environment*, 858, 159815.
10. Durán, A., Monteagudo, J., Carnicer, A., Ruiz-Murillo, M. (2011). Photo-Fenton mineralization of synthetic municipal wastewater effluent containing acetaminophen in a pilot plant. *Desalination*, 270(1–3), 124–129.
11. Fang, J., Zhan, L., Ok, Y. S., Gao, B. (2018). Mini-review of potential applications of hydrochar derived from hydrothermal carbonization of biomass. *Journal of Industrial and Engineering Chemistry*, 57, 15–21. <https://doi.org/https://doi.org/10.1016/j.jiec.2017.08.026>
12. González-Hourcade, M., dos Reis, G. S., Grimm, A., Lima, E. C., Larsson, S. H., Gentili, F. G. (2022). Microalgae biomass as a sustainable precursor to produce nitrogen-doped biochar for efficient removal of emerging pollutants from aqueous media. *Journal of Cleaner Production*, 348, 131280.
13. Hamid, Y., Liu, L., Usman, M., Naidu, R., Haris, M., Lin, Q.,... Yang, X. (2022). Functionalized biochars: Synthesis, characterization, and applications for removing trace elements from water. *Journal of Hazardous materials*, 437, 129337.
14. Jain, M., Kiran, P. S., Ghosal, P. S., Gupta, A. K. (2023). Development of microbial fuel cell integrated constructed wetland (CMFC) for removal of paracetamol and diclofenac in hospital wastewater. *Journal of Environmental Management*, 344, 118686.
15. Jin, H., Capareda, S., Chang, Z., Gao, J., Xu, Y., Zhang, J. (2014). Biochar pyrolytically produced from municipal solid wastes for aqueous As(V) removal: adsorption property and its improvement with KOH activation. *Bioresource Technology*, 169, 622–629.
16. Jung, C., Oh, J., Yoon, Y. (2015). Removal of acetaminophen and naproxen by combined coagulation and adsorption using biochar: influence of combined sewer overflow components. *Environmental Science and Pollution Research*, 22, 10058–10069.
17. Karaman, R., Khamis, M., Abbadi, J., Amro, A.,

- Curie, M., Ayyad, I.,...Nir, S. (2016). Paracetamol biodegradation by activated sludge and photocatalysis and its removal by a micelle–clay complex, activated charcoal, and reverse osmosis membranes. *Environmental Technology*, 37(19), 2414–2427.
18. Kerkhoff, C. M., da Boit Martinello, K., Franco, D. S., Netto, M. S., Georgin, J., Foletto, E. L.,... Dotto, G. L. (2021). Adsorption of ketoprofen and paracetamol and treatment of a synthetic mixture by novel porous carbon derived from *Butia capitata* endocarp. *Journal of Molecular Liquids*, 339, 117184.
19. Lee, Y.-G., Shin, J., Kwak, J., Kim, S., Son, C., Kim, G.-Y.,...Chon, K. (2021). Enhanced adsorption capacities of fungicides using peanut shell biochar via successive chemical modification with KMnO_4 and KOH . *Separations*, 8(4), 52.
20. Lessa, E. F., Nunes, M. L., Fajardo, A. R. (2018). Chitosan/waste coffee-grounds composite: An efficient and eco-friendly adsorbent for removal of pharmaceutical contaminants from water. *Carbohydrate Polymers*, 189, 257–266.
21. Liu, Z., Li, P., Chang, C., Wang, X., Song, J., Fang, S., Pang, S. (2022). Influence of metal chloride modified biochar on products characteristics from biomass catalytic pyrolysis. *Energy*, 250, 123776.
22. Loc, T. T., Dat, N. D., Tran, H. N. (2023). Nano-sized hematite-assembled carbon spheres for effectively adsorbing paracetamol in water: Important role of iron. *Korean Journal of Chemical Engineering*, 40(12), 3029–3038. <https://doi.org/10.1007/s11814-021-1013-z>
23. Lung, I., Soran, M.-L., Stegarescu, A., Opris, O., Gutoiu, S., Leostean, C.,...Porav, A. S. (2021). Evaluation of $\text{CNT-COOH/MnO}_2/\text{Fe}_3\text{O}_4$ nanocomposite for ibuprofen and paracetamol removal from aqueous solutions. *Journal of Hazardous materials*, 403, 123528.
24. Maneewong, Y., Chaemchuen, S., Verpoort, F., Klomkliang, N. (2022). Paracetamol removal from water using N-doped activated carbon derived from coconut shell: Kinetics, equilibrium, cost analysis, heat contributions, and molecular-level insight. *Chemical Engineering Research and Design*, 185, 163–175.
25. Nasr, O., Mohamed, O., Al-Shirbini, A.-S., Abdel-Wahab, A.-M. (2019). Photocatalytic degradation of acetaminophen over Ag, Au and Pt loaded TiO_2 using solar light. *Journal of Photochemistry and Photobiology A: Chemistry*, 374, 185–193.
26. Natarajan, R., Banerjee, K., Kumar, P. S., Somanna, T., Tannani, D., Arvind, V.,...Vaidyanathan, V. K. (2021). Performance study on adsorptive removal of acetaminophen from wastewater using silica microspheres: Kinetic and isotherm studies. *Chemosphere*, 272, 129896.
27. Negarestani, M., Motamedi, M., Kashtiaray, A., Khadir, A., Sillanpää, M. (2020). Simultaneous removal of acetaminophen and ibuprofen from underground water by an electrocoagulation unit: Operational parameters and kinetics. *Groundwater for Sustainable Development*, 11, 100474.
28. Nguyen, D. T., Tran, H. N., Juang, R.-S., Dat, N. D., Tomul, F., Ivanets, A.,...Chao, H.-P. (2020). Adsorption process and mechanism of acetaminophen onto commercial activated carbon. *Journal of Environmental Chemical Engineering*, 8(6), 104408.
29. Patel, M., Kumar, R., Pittman Jr, C. U., Mohan, D. (2021). Ciprofloxacin and acetaminophen sorption onto banana peel biochars: Environmental and process parameter influences. *Environmental Research*, 201, 111218.
30. Peiris, C., Nayanathara, O., Navarathna, C. M., Jayawardhana, Y., Nawalage, S., Burk, G.,...Kaumal, M. (2019). The influence of three acid modifications on the physicochemical characteristics of tea-waste biochar pyrolyzed at different temperatures: a comparative study. *Rsc Advances*, 9(31), 17612–17622.
31. Peng, H., Gao, P., Chu, G., Pan, B., Peng, J., Xing, B. (2017). Enhanced adsorption of Cu (II) and Cd (II) by phosphoric acid-modified biochars. *Environmental Pollution*, 229, 846–853.
32. Peng, Y., Sun, Y., Hanif, A., Shang, J., Shen, Z., Hou, D.,...Tsang, D. C. (2021). Design and fabrication of exfoliated Mg/Al layered double hydroxides on biochar support. *Journal of Cleaner Production*, 289, 125142.
33. Peralta-Hernández, J. M., Brillas, E. (2023). A critical review over the removal of paracetamol (acetaminophen) from synthetic waters and real wastewaters by direct, hybrid catalytic, and sequential ozonation processes. *Chemosphere*, 313, 137411.
34. Pimentel-Almeida, W., Itokazu, A. G., Bazani, H. A. G., Maraschin, M., Rodrigues, O. H. C., Corrêa, R. G.,...Moresco, R. (2023). Beach-cast *Sargassum cymosum* macroalgae: biochar production and apply to adsorption of Acetaminophen in batch and fixed-bed adsorption processes. *Environmental Technology*, 44(7), 974–987.
35. Qasim, H. M., Abudi, Z. N., Alzubaidi, L. A. (2023). Cobalt ion removal using magnetic biochar obtained from *Conocarpus erectus* leaves. *Biomass Conversion and Biorefinery*, 13(18), 16865–16875.
36. Quesada, H. B., Cusioli, L. F., de O Bezerra, C., Baptista, A. T., Nishi, L., Gomes, R. G., Bergamasco, R. (2019). Acetaminophen adsorption using a low-cost adsorbent prepared from modified residues of *Moringa oleifera* Lam. seed husks. *Journal of Chemical Technology & Biotechnology*, 94(10), 3147–3157.
37. Qutob, M., Hussein, M. A., Alamry, K. A., Rafatullah, M. (2022). A review on the degradation of acetaminophen by advanced oxidation process: pathway, by-products, biotoxicity, and density

- functional theory calculation. *Rsc Advances*, 12(29), 18373–18396.
38. Ramasamy, B., Jeyadharman, J., Chinnaiyan, P. (2021). Novel organic assisted Ag-ZnO photocatalyst for atenolol and acetaminophen photocatalytic degradation under visible radiation: performance and reaction mechanism. *Environmental Science and Pollution Research*, 28(29), 39637–39647.
39. Sellaoui, L., Abdulaziz, F., Chebaane, S., Manai, L., Azhary, A., Alsehli, A. H.,...Erto, A. (2023). Adsorption of pharmaceutical pollutants on activated carbon: Physicochemical assessment of the adsorption mechanism via advanced modelling. *Journal of Molecular Liquids*, 389, 122929.
40. Utami, T. S., Arbiandi, R., Hidayatullah, I. M., Yusupandi, F., Hamdan, M., Putri, N. F.,...Boopathy, R. (2024). Paracetamol degradation in a dual-chamber rectangular membrane bioreactor using microbial fuel cell system with a microbial consortium from sewage sludge. *Case Studies in Chemical and Environmental Engineering*, 9, 100551.
41. Wang, Y., Kang, J., Jiang, S., Li, H., Ren, Z., Xu, Q.,...Zhang, Y. (2020). A composite of Ni-Fe-Zn layered double hydroxides/biochar for atrazine removal from aqueous solution. *Biochar*, 2, 455–464.
42. Wen, Q., Chen, Y., Rao, X., Yang, R., Zhao, Y., Li, J.,...Liang, Z. (2022). Preparation of magnesium Ferrite-Doped magnetic biochar using potassium ferrate and seawater mineral at low temperature for removal of cationic pollutants. *Bioresource Technology*, 350, 126860.
43. Xue, L., Gao, B., Wan, Y., Fang, J., Wang, S., Li, Y.,...Yang, L. (2016). High efficiency and selectivity of MgFe-LDH modified wheat-straw biochar in the removal of nitrate from aqueous solutions. *Journal of the Taiwan Institute of Chemical Engineers*, 63, 312–317. <https://doi.org/https://doi.org/10.1016/j.jtice.2016.03.021>
44. Zhang, H., Su, L., Cheng, C., Cheng, H., Chang, M., Liu, F.,...Oh, K. (2022). A new type of calcium-rich biochars derived from spent mushroom substrates and their efficient adsorption properties for cationic dyes. *Frontiers in Bioengineering and Biotechnology*, 10, 1007630.
45. Zhang, Z., Li, Y., Zong, Y., Yu, J., Ding, H., Kong, Y.,...Ding, L. (2022). Efficient removal of cadmium by salts modified-biochar: Performance assessment, theoretical calculation, and quantitative mechanism analysis. *Bioresource Technology*, 361, 127717.
46. Zhu, H., Chen, T., Liu, J., Li, D. (2018). Adsorption of tetracycline antibiotics from an aqueous solution onto graphene oxide/calcium alginate composite fibers [10.1039/C7RA11964J]. *RSC Advances*, 8(5), 2616–2621. <https://doi.org/10.1039/C7RA11964J>